AGU PUBLICATIONS

Geophysical Research Letters

RESEARCH LETTER
10.1002/2015GL064363

Key Points:
- Low-frequency earthquakes (LFEs) found throughout southern Cascadia
- LFE families discovered on the Maacama and Bucknell Creek Faults
- Shallow earthquake swarms on these faults may be driven by deeper slow slip

Correspondence to:
A. P. Plourde,
aplourde@eos.ubc.ca

Citation:
Plourde, A. P., M. G. Bostock, P. Audet, and A. M. Thomas (2015), Low-frequency earthquakes at the southern Cascadia margin, *Geophys. Res. Lett.*, *42*, 4849–4855, doi:10.1002/2015GL064363.

Received 29 APR 2015
Accepted 15 JUN 2015
Accepted article online 18 JUN 2015
Published online 30 JUN 2015

Low-frequency earthquakes at the southern Cascadia margin

Alexandre P. Plourde[1], Michael G. Bostock[1], Pascal Audet[2], and Amanda M. Thomas[3]

[1]Department of Earth, Ocean, and Atmospheric Sciences, University of British Columbia, Vancouver, British Columbia, Canada, [2]Department of Earth and Environmental Science, University of Ottawa, Ottawa, Ontario, Canada, [3]Department of Geological Sciences, University of Oregon, Eugene, Oregon, USA

Abstract We use seismic waveform data from the Mendocino Experiment to detect low-frequency earthquakes (LFEs) beneath Northern California during the April 2008 tremor-and-slip episode. In southern Cascadia, 59 templates were generated using iterative network cross correlation and stacking and grouped into 34 distinct LFE families. The main front of tremor epicenters migrates along strike at 9 km d^{-1}; we also find one instance of rapid tremor reversal, observed to propagate in the opposite direction at 10–20 km h^{-1}. As in other regions of Cascadia, LFE hypocenters from this study lie several kilometers above a recent plate interface model. South of Cascadia, LFEs were discovered on the Maacama and Bucknell Creek faults. The Bucknell Creek Fault may be the youngest fault yet observed to host LFEs. These fault zones also host shallow earthquake swarms with repeating events that are distinct from LFEs in their spectral and recurrence characteristics.

1. Introduction

It is now widely agreed upon that repeating low-frequency earthquakes (LFEs) are the source of most if not all tectonic tremor — the two terms refer to a single natural phenomenon. Throughout the paper we use "LFEs" to refer to individual events and "tremor" to refer to them more generally. Tremor occurs as a product of slow-slip downdip of the seismogenic zone in subduction zones [*Obara*, 2002; *Rogers and Dragert*, 2003] and major strike-slip faults [*Shelly et al.*, 2009; *Aiken et al.*, 2013]. When it was first observed in subduction zones, many predicted the source to be fluid flow, given its similarity to volcanic tremor. In most subduction zones where tremor has been documented, it has been observed to coincide with a low-velocity zone (LVZ) displaying high v_p/v_s ratio. Most have interpreted the LVZ to represent a region with near-lithostatic pore fluid pressures in the upper oceanic crust [*Shelly et al.*, 2006; *Audet et al.*, 2009; *Song et al.*, 2009] or subducted sediments [*Calvert et al.*, 2011]. *McCrory et al.* [2012] suggested that beneath Oregon it could represent hydrated rocks in the overriding plate. LFE focal mechanisms indicate that they result from shear slip [*Ide et al.*, 2007; *Royer and Bostock*, 2014], leading most to believe that they represent slip on or near the plate interface. Together with theoretical and numerical modeling [*Beeler et al.*, 2013; *Yamashita*, 2013; *Gershenzon and Bambakidis*, 2014], a growing archive of observations related to LFE waveforms, recurrence, and migration are continually refining our understanding of tremor.

In Cascadia most LFEs occur in ~2–3 week long, geodetically detectable episodes of slow slip that recur every 10–20 months, a phenomenon termed episodic tremor and slip (ETS) [*Rogers and Dragert*, 2003]. ETS recurrence intervals are segmented along major geological domains. Under the Klamath zone in southern Cascadia, ETS repeats approximately every 10 months [*Brudzinski and Allen*, 2007], whereas farther north between the Siletzia and Wrangellia terranes recurrence intervals are approximately 19 and 14 months, respectively. *Audet and Bürgmann* [2014] hypothesized that variations in recurrence interval result from varying silica content in the overriding crust; quartz precipitation above the plate interface reduces permeability, allowing fluid pressures to build more quickly. Along transform faults such as the San Andreas Fault, episodic tremor has also been observed, but with a typical recurrence interval of 1–4 months [*Guilhem and Nadeau*, 2012].

We use data from the EarthScope Flexible Array Mendocino Experiment, which was deployed between July 2007 and December 2009 over northern California, and recorded during the April 2008 ETS episode. This array provides a unique opportunity to study LFEs in the region, as permanent stations are too sparsely distributed to detect them effectively. First, we detect and locate LFE families in southern Cascadia, and we compare

their locations to a catalog of double-difference relocated earthquakes from *Waldhauser and Schaff* [2008] and the *McCrory et al.* [2012] plate interface model. Second, we observe shallow LFE families immediately south of the subduction zone and compare their properties to LFEs within the subduction zone and local earthquake swarms.

2. Methods

Data were collected for 25 stations from the Mendocino Experiment, as well as 7 permanent stations from the Northern California Seismic Network, for the period of 21 March to 30 April 2008. Data were filtered between 1.5 and 9 Hz before LFEs were found using a combination of autodetection methods [*Savard and Bostock*, 2015] and visual identification; windows of 60 s around these LFEs were used as initial templates. Higher signal-to-noise ratio (SNR) LFE signals were then recovered using iterative network cross correlation [*Gibbons and Ringdal*, 2006; *Shelly et al.*, 2007] to find and stack repeats of the initial template LFE. As this study spans a larger area than previous implementations of this method, we used initial hypocentral estimates to create a station-dependent taper window—this allowed us to use a short window of 12 s.

Phase-weighted stacking was employed until the final iteration of network cross correlation and stacking. This technique has been demonstrated to increase SNR and produce more LFE detections [*Thurber et al.*, 2014], but in this study we found linear stacking to generate more detections in later iterations, once the template had a sufficiently high SNR. For hypocentral location, we used a one-dimensional velocity model modified from *Verdonck and Zandt* [1994].

Final templates were tested for uniqueness using two distinct methods. First, the number of shared detections times was computed, allowing for a lag of up to 25 s since the signal can be shifted within the 60 s template. As this method requires times to be shared to the nearest sample ($\Delta t = 0.025$ s), the templates were considered to originate from the same family if >10% of detections were shared. As a second test, cross-correlation coefficients were computed for each template pair, using only stations for which a phase was picked; again, this allowed for a lag of up to 25 s. A correlation coefficient >0.3 was considered to suggest templates originated from the same family.

3. Southern Cascadia

A total of 59 initial templates from Cascadia produced waveforms sufficiently clear to be picked. These 59 templates were found to represent 34 distinct LFE families. These families comprised 9900 LFEs, or a mean of 290 per family, with 870 as the largest number of detections in a single family.

LFE families were plotted in plan view (Figure 1) along with the stations used for this study, earthquakes from the *Waldhauser and Schaff* [2008] catalog, and the plate interface model from *McCrory et al.* [2012]. The Cascadia LFEs extend from 40°N to 41.8°N, but this northern limit may simply reflect a gap in station coverage in southern Oregon. Hypocentral depths range from 28 km to 47 km, a larger distribution than in northern Cascadia [*Bostock et al.*, 2012] or Japan [*Shelly et al.*, 2007].

The *McCrory et al.* [2012] model is the most recent and the most detailed plate interface model in Cascadia. It relies primarily on the top of the Wadati-Benioff zone to mark the top of the slab, with active source and receiver function profiles employed as supplemental data where seismicity is sparse. *Audet et al.* [2010] produced a plate interface model based on the location of the LVZ from stacked receiver functions but had low station density in Northern California and could not resolve the slab curvature in the region.

LFEs and earthquakes from Cascadia are shown in cross section in Figure 2. In order to display all the data on one plot while avoiding projection errors, all events were plotted relative to the *McCrory et al.* [2012] plate interface model. First, the plate interface was plotted for a midlatitude east-west profile. For each LFE and each catalog earthquake a *model depth* was found, meaning the depth of the plate interface model beneath it. On the cross section the events were plotted at their true depth, but at the easting that corresponds to the correct model depth. There are large earthquakes clusters both in the western, shallow, part of the slab and in the overriding plate; *McCrory et al.* [2012] associate the former with flexure in the slab and the latter with a detached piece of hydrated oceanic crust. Intraplate seismicity is abundant in the shallow part of the slab but becomes sparse at the onset of the tremor-producing zone, with very few deeper events.

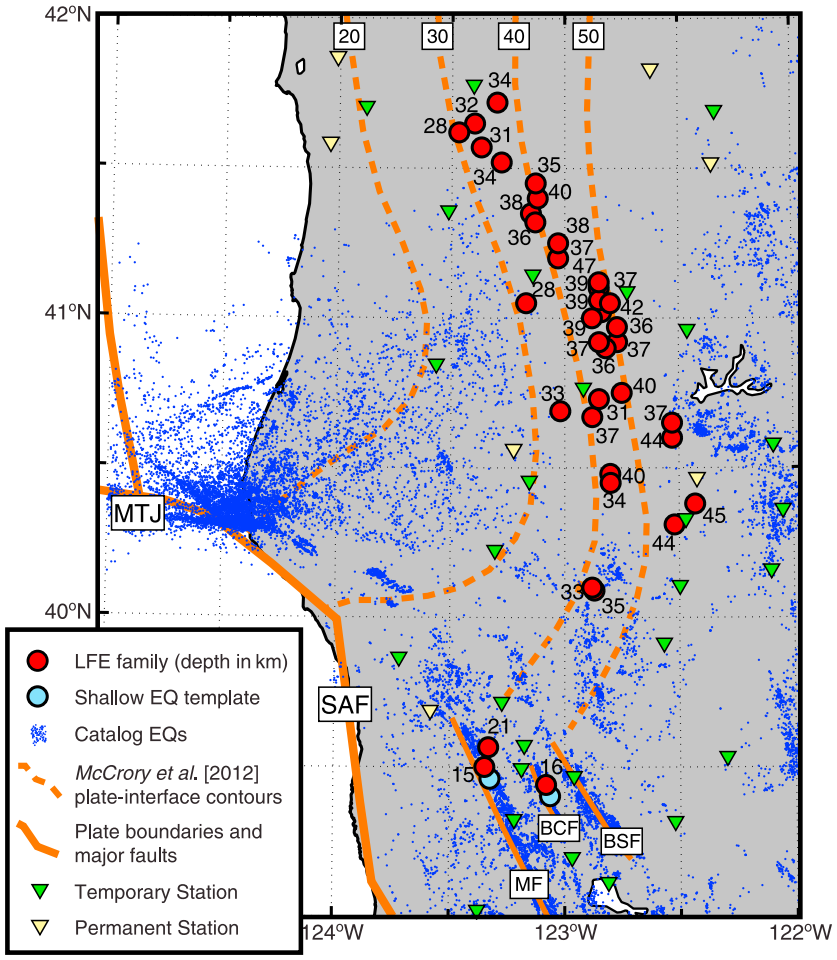

Figure 1. LFE families are plotted in plan view along with earthquakes and the 20, 30, 40, and 50 km depth contours from the *McCrory et al.* [2012] plate interface model. Each LFE family is labeled with its depth in kilometers. The southern LFE families at 15 km and 21 km depth lie on the Maacama Fault, while the family at 16 km depth lies on Bucknell Creek Fault. The location of the two shallow earthquakes used as templates for network cross correlation is indicated with blue circles. MTJ: Mendocino Triple Junction, SAF: San Andreas Fault, MF: Maacama Fault, BCF: Bucknell Creek Fault, BSF: Bartlett Springs Fault.

Many templates exhibited complicated waveforms that proved difficult to pick compared to those from the southern Vancouver Island region [*Bostock et al.*, 2012]. Even at relatively high SNR, the direct *P* wave often lacks clear, impulsive arrivals, adding some uncertainty to source depths. We suggest that this is due to structural complexity in the overriding crust, and in Figure 2 we assume that this uncertainty is responsible for much of depth scatter in LFEs. Nevertheless, LFE hypocenters consistently lie above the *McCrory et al.* [2012]

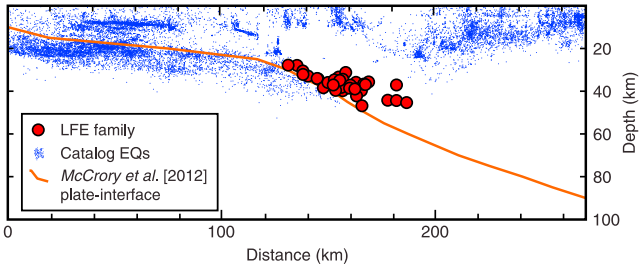

Figure 2. A cross section through southern Cascadia with LFEs (red circles) and regular earthquakes (blue dots) drawn relative to the *McCrory et al.* [2012] plate interface model. Although there is some scatter in the LFE depths, they lie distinctly above the model plate interface.

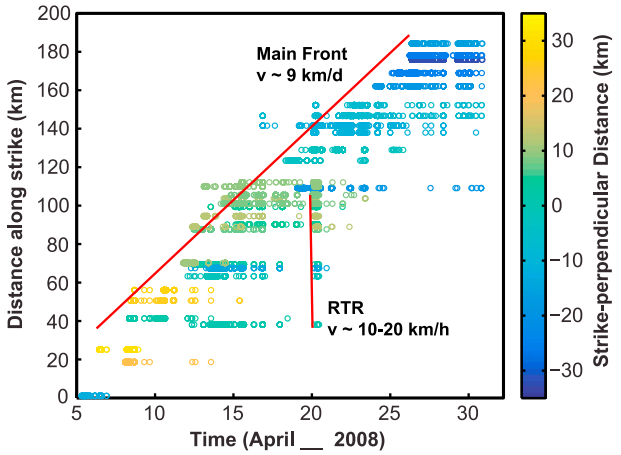

Figure 3. A time-distance plot of LFE epicenters in southern Cascadia. Distance is measured parallel to the strike of the *McCrory et al.* [2012] plate interface model, with positive being approximately NNW. The across-strike distance is shown in the color scale, with positive corresponding to ENE. The main front is seen to travel NNW at approximately 9 km d^{-1}. One occurrence of rapid tremor reversal stands out, traveling SSE at 10–20 km h^{-1}.

plate interface model. As LFEs represent a zone of active shear slip, this may suggest that the model is biased deep and that Wadati-Benioff earthquakes are not occurring in the upper few kilometers of the subducting slab. We cannot, however, rule out that the bias is not related to the velocity model used to locate the LFEs.

The vast majority of LFEs occur in large bursts of tremor that last several minutes to several hours. Subsequent bursts of the same family often occur in the hours and days following the initial burst. Only on a few occasions is a burst separated from another of the same family by more than 2 days, and these are generally associated with rapid tremor reversals (RTRs). This term is used by *Houston et al.* [2011] to describe high-velocity tremor migration in the direction opposite to the main front within an ETS episode; they observe velocities of 7–17 km h^{-1}, 1–2 orders of magnitude faster than the main front. In southern Cascadia we observe the main front to migrate NNW—approximately along strike of the plate interface—at 9 km d^{-1}, with one RTR observed to travel SSE at 10–20 km h^{-1} (Figure 3).

A distinct spatial anticorrelation between LFEs and regular earthquakes stands out in Figure 1. A similar observation was made by *Boyarko and Brudzinski* [2010] for tremor, who suggested that continual slow slip on the plate interface reduces stress in the overriding plate, preventing regular earthquakes from occurring.

4. The San Andreas Fault System

Three LFE families were found well south of the subducting Gorda Plate, in the San Andreas Fault zone. Two of these families appears to lie on the Maacama Fault (39.50°N, 123.36°W, 15 km depth; 39.56°N, 123.33°W, 21 km depth), which *Castillo and Ellsworth* [1993] mapped as dipping 70°NE in this region, using earthquake hypocenters. The other family lies on the northern Bucknell Creek Fault (39.45°N, 123.10°W, 16 km depth), which accommodates shear stress between the western Maacama and eastern Bartlett Springs Fault zones [*Thomas et al.*, 2013]. The shallow portion of the fault is extremely young, ~1 Myr, possibly making this the youngest fault known to host LFEs. It is possible, however, that the deep sections from the fault are inherited from older fabrics related to Farallon subduction.

We observe the Maacama and Bucknell Creek LFE families for 2 months (1 March to 30 April 2008) and find tremor bursts throughout the whole duration, separated by as little as 1 day, but as many as 17 days. The Maacama Fault LFE families had 869 and 302 repeats in this time span, respectively, and the Bucknell Creek Fault family had 325. The setting and behavior of these LFEs resembles those documented by *Shelly et al.* [2009] and *Shelly* [2010] on the San Andreas Fault, between 16 and 29 km in depth. While we do not believe tremor on the Maacama or Bucknell Creek faults has been previously documented, *Gomberg et al.* [2008] did observe tremor on several similar faults in central and southern California, triggered by surface waves from the 2002 Denali earthquake.

During our search for LFEs, we also noted distinct families of other repeating earthquakes during this time period, on the Macaama and Bucknell Creek faults at depths of 7 to 11 km. These earthquakes recur quasiperiodically as single events or in small groups, unlike deeper LFEs that occur as part of large tremor bursts. These contrasting behaviors are displayed in network correlation coefficients for a single day in Figures 4a and 4b. The contrast is also apparent in Figure 4c, which displays the cumulative number of detections for LFE and shallow earthquake templates on each fault. The tremor burst behavior of LFEs results in staircase-like

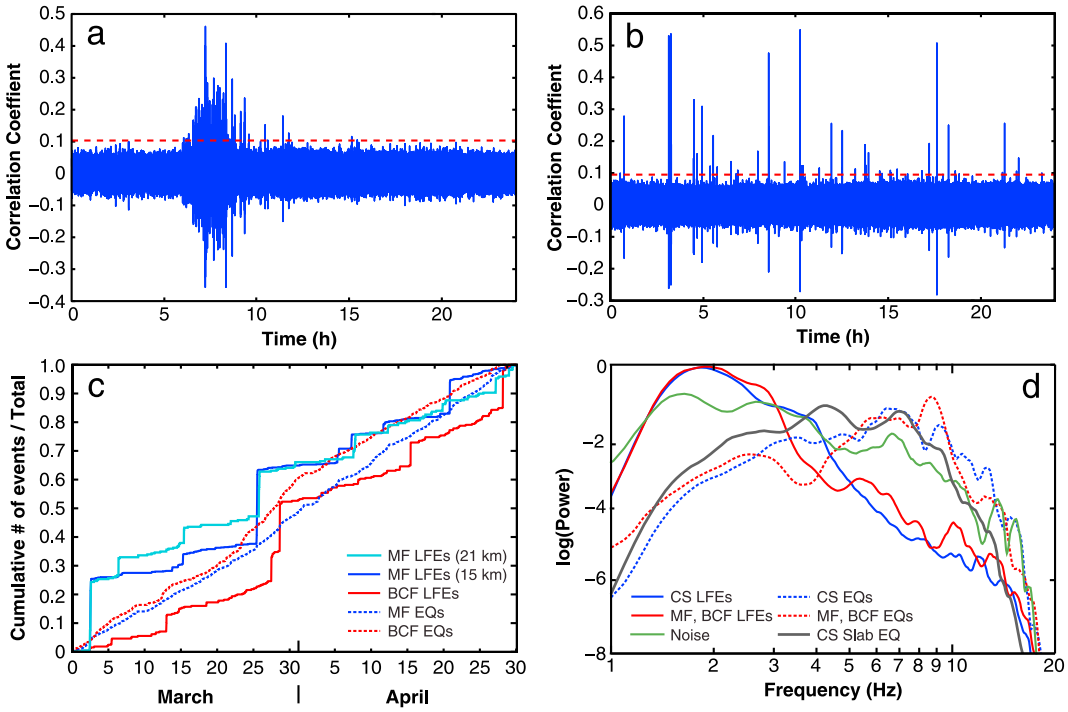

Figure 4. Network cross-correlation coefficients for 1 day from (a) the LFE family at 15 km depth on the Maacama Fault and (b) repeating earthquakes at 9 km depth on the Maacama Fault. (c) The cumulative number of detected LFEs and shallow earthquakes on both the Maacama and Bucknell Creek Faults, relative to the total number of detections from their respective templates. The two Maacama Fault families are distinguished by their depth. Tremor bursts give the LFE data a staircase-like appearance, contrasting the more continuous shallow earthquake activity. (d) Multitaper spectra of velocity for LFEs and repeating crustal earthquakes from both the Cascadia subduction zone and Maacama Fault region. Each spectra was normalized so that relative frequency content, rather than total power, can be easily compared. We used averages from three different events over several stations and 8 s windows starting 1 s before the *S* arrival. The LFE spectra are both distinctly elevated in the 1.5 to 4 Hz range, while energy in the crustal earthquakes is peaked at 5 to 10 Hz. The spectrum of intraslab earthquakes, shown in grey, is also richer in high frequencies than the LFEs. Each style of event has a distinct spectra from ambient noise, shown in green.

progression, whereas the shallow earthquakes have a more linear trend. The earthquake templates each generated over 1000 detections, but most of these were not true repeating events. Since these earthquakes have much greater SNR than LFEs, detections were often made when the largest portions of the *S* wave were aligned, even if *P* arrival times indicated the two events originate from significantly different locations. A detection in this case indicates that the events are part of the same earthquake swarm [*Thomas et al.*, 2013], but their locations and source mechanisms can vary more than we expect for LFEs belonging to the same family. It is plausible that these earthquake swarms are related to larger-scale slow slip on deeper sections of the fault. *Lohman and McGuire* [2007] proposed a similar mechanism in which very shallow earthquakes are triggered by aseismic creep on the southern San Andreas Fault.

Normalized power spectra of the LFEs and shallow earthquakes, computed using a multitaper approach, are plotted in Figure 4d between 1 Hz and 20 Hz. LFEs from both Cascadia and the southern faults are found to have energy peaked between 1.5 to 4 Hz, while the repeating earthquakes have energy peaked at 5 and 10 Hz. To ensure the differences are characteristic of the sources and not due to high-frequency attenuation of LFE signals, we examine the spectra of two intraslab earthquakes. The earthquakes were M ~3 and occurred near 30 km depth, yet had spectra more similar to the shallow earthquakes. Both the LFEs and regular earthquakes are shown to have distinct spectra from ambient noise. The LFE spectra observed on the Maacama and Bucknell Creek faults are similar to those observed in subduction zones but peak at lower frequencies than San Andreas Fault LFEs, for which energy is concentrated above 3 Hz [*Nadeau and Dolenc*, 2005; *Shelly et al.*, 2009].

Seismic reflection surveys indicate that the Maacama fault cuts through the entire crust to the mantle, which is only 25 km deep in the region [*Beaudoin et al.*, 1996]; this may be an important factor in tremor production.

As the Mendocino triple junction and the edge of the Juan de Fuca slab migrated northward [*Furlong*, 1993], upwelling asthenosphere heated a mantle wedge that was previously cooled by the subducting plate. *Kirby et al.* [2014] suggest that higher temperatures caused a serpentinized portion of the mantle wedge to dehydrate, forming olivine and talc. Water released from the mantle could then migrate upward into deep crustal fault systems and play a crucial role in the generation of both tremor and regular seismicity through production of high pore fluid pressures. Further evidence for the presence of abundant fluids underlying the Maacama and Bartlett Springs fault zones comes from the work of *Levander et al.* [1998] who noted anomalous reflectors in the region and hypothesized the presence of active mafic intrusives in the lower crust.

5. Conclusions

This study is the first documentation of extensive LFE activity in southern Cascadia. LFE hypocenters are consistently a few kilometers above the *McCrory et al.* [2012] plate interface model. Additional families of LFEs were discovered on the Maacama Fault and Bucknell Creek Fault, at the northern edge of the San Andreas fault system. These events have similar recurrence behaviors to those found on the San Andreas Fault proper, differing from those found in Cascadia. The Bucknell Creek Fault may be the youngest fault found to host LFEs. Shallow earthquake swarms on these fault systems were found to have distinct spectra and recurrence properties from LFEs. We speculate that these swarms are influenced by slow slip on deeper sections of the fault.

Acknowledgments

The data used in this study come from the EarthScope Mendocino Experiment, funded by the National Science Foundation (U.S.), and from the Northern California Seismic Network deployed by the Berkeley Seismological Laboratory. Data were accessed through the Incorporated Research Institutions for Seismology Data Management Center, doi:10.7914/SN/XQ_2007. This work was funded by the Natural Science and Engineering Research Council through discovery grants to M.G.B and P.A., as well as a Canada Graduate Scholarship to A.P.P.; A.M.T. was supported by NSF EAR-PF award 1249775. We thank an anonymous reviewer whose comments improved this paper.

The Editor thanks Joan Gomberg for her assistance in evaluating this paper.

References

Aiken, C., Z. Peng, and K. Chao (2013), Tremors along the Queen Charlotte Margin triggered by large teleseismic earthquakes, *Geophys. Res. Lett.*, *40*, 829–834, doi:10.1002/grl.50220.

Audet, P., and R. Bürgmann (2014), Possible control of subduction zone slow-earthquake periodicity by silica enrichment, *Nature*, *509*, 389–392, doi:10.1038/nature13391.

Audet, P., M. G. Bostock, N. I. Christensen, and S. M. Peacock (2009), Seismic evidence for overpressured subducted oceanic crust and megathrust fault sealing, *Nature*, *457*, 76–78, doi:10.1038/nature07650.

Audet, P., M. G. Bostock, D. C. Boyarko, M. R. Brudzinski, and R. M. Allen (2010), Slab morphology in the Cascadia fore arc and its relation to episodic tremor and slip, *J. Geophys. Res.*, *115*, B00A16, doi:10.1029/2008JB006053.

Beaudoin, B. C., et al. (1996), Transition from slab to slabless: Results from the 1993 Mendocino triple junction seismic experiment, *Geology*, *24*, 195–199, doi:10.1130/0091-7613.

Beeler, N. M., A. Thomas, R. Bürgmann, and D. Shelly (2013), Inferring fault rheology from low-frequency earthquakes on the San Andreas, *J. Geophys. Res. Solid Earth*, *118*, 5976–5990, doi:10.1002/2013JB010118.

Bostock, M. G., A. A. Royer, E. H. Hearn, and S. M. Peacock (2012), Low frequency earthquakes below southern Vancouver Island, *Geochem. Geophys. Geosyst.*, *13*, Q11007, doi:10.1029/2012GC004391.

Boyarko, D. C., and M. R. Brudzinski (2010), Spatial and temporal patterns of nonvolcanic tremor along the southern Cascadia subduction zone, *J. Geophys. Res.*, *115*, B00A22, doi:10.1029/2008JB006064.

Brudzinski, M. R., and R. M. Allen (2007), Segmentation in episodic tremor and slip all along Cascadia, *Geology*, *35*, 907–910, doi:10.1130/G23740A.1.

Calvert, A. J., L. A. Preston, and A. M. Farahbod (2011), Sedimentary underplating at the Cascadia mantle-wedge corner revealed by seismic imaging, *Nat. Geosci.*, *4*, 545–548, doi:10.1038/ngeo1195.

Castillo, D. A., and W. L. Ellsworth (1993), Seismotectonics of the San Andreas Fault system between Point Arena and Cape Mendocino in northern California: Implications for the development and evolution of a young transform, *J. Geophys. Res.*, *98*, 6543–6560.

Furlong, K. P. (1993), Thermal-rheologic evolution of the upper mantle and the development of the San Andreas Fault system, *Tectonophysics*, *223*, 149–164, doi:10.1016/0040-1951(93)90162-D.

Gershenzon, N. I., and G. Bambakidis (2014), Model of deep nonvolcanic tremor. Part I: Ambient and triggered tremor, *Bull. Seismol. Soc. Am.*, *104*, 2073–2090, doi:10.1785/0120130234.

Gibbons, S. J., and F. Ringdal (2006), The detection of low magnitude seismic events using array-based waveform correlation, *Geophys. J. Int.*, *165*, 149–166, doi:10.1111/j.1365-246X.2006.02865.x.

Gomberg, J., J. L. Rubinstein, Z. Peng, K. C. Creager, J. E. Vidale, and P. Bodin (2008), Widespread triggering of nonvolcanic tremor in California, *Science*, *319*, 173, doi:10.1126/science.1149164.

Guilhem, A., and R. M. Nadeau (2012), Episodic tremors and deep slow-slip events in central California, *Earth Planet. Sci. Lett.*, *357–358*, 1–10, doi:10.1016/j.epsl.2012.09.028.

Houston, H., B. G. Delbridge, A. G. Wech, and K. C. Creager (2011), Rapid tremor reversals in Cascadia generated by a weakened plate interface, *Nat. Geosci.*, *4*, 404–409, doi:10.1038/ngeo1157.

Ide, S., D. R. Shelly, and G. C. Beroza (2007), Mechanism of deep low frequency earthquakes: Further evidence that deep non-volcanic tremor is generated by shear slip on the plate interface, *Geophys. Res. Lett.*, *34*, L03308, doi:10.1029/2006GL028890.

Kirby, S., K. Wang, and T. M. Brocher (2014), A possible deep, long-term source for water in the northern San Andreas Fault system: A ghost of Cascadia subduction past?, *Earth Planets Space*, *66*, 67, doi:10.1186/1880-5981-66-67.

Levander, A., T. J. Henstock, A. S. Meltzer, B. C. Beaudoin, A. M. Trehu, and S. L. Klemperer (1998), Fluids in the lower crust following Mendocino triple junction migration: Active basaltic intrusion?, *Geology*, *26*, 171–174, doi:10.1130/0091-7613(1998)026.

Lohman, R. B., and J. J. McGuire (2007), Earthquake swarms driven by aseismic creep in the Salton Trough, California, *J. Geophys. Res.*, *112*, B04405, doi:10.1029/2006JB004596.

McCrory, P. A., J. L. Blair, F. Waldhauser, and D. H. Oppenheimer (2012), Juan de Fuca slab geometry and its relation to Wadati-Benioff zone seismicity, *J. Geophys. Res.*, *117*, B09306, doi:10.1029/2012JB009407.

Nadeau, R. M., and D. Dolenc (2005), Nonvolcanic tremors deep beneath the San Andreas Fault, *Science*, *307*, 389, doi:10.1126/science.1107142.

Obara, K. (2002), Nonvolcanic deep tremor associated with subduction in southwest Japan, *Science*, *296*, 1679–1681, doi:10.1126/science.1070378.

Rogers, G., and H. Dragert (2003), Episodic tremor and slip on the Cascadia subduction zone: The chatter of silent slip, *Science*, *300*, 1942–1943, doi:10.1126/science.1084783.

Royer, A. A., and M. Bostock (2014), A comparative study of low frequency earthquake templates in northern Cascadia, *Earth Planet. Sci. Lett.*, *402*, 247–256, doi:10.1016/j.epsl.2013.08.040.

Savard, G., and M. G. Bostock (2015), High resolution detection and location of low frequency earthquakes using cross-station and cross-detection correlation, *Bull. Seismol. Soc. Am.*, *105*, doi:10.1785/0120140301, in press.

Shelly, D. R. (2010), Periodic, chaotic, and doubled earthquake recurrence intervals on the deep San Andreas Fault, *Science*, *328*, 1385–1388, doi:10.1126/science.1189741.

Shelly, D. R., G. C. Beroza, S. Ide, and S. Nakamula (2006), Low-frequency earthquakes in Shikoku, Japan, and their relationship to episodic tremor and slip, *Nature*, *442*, 188–191, doi:10.1038/nature04931.

Shelly, D. R., G. C. Beroza, and S. Ide (2007), Non-volcanic tremor and low-frequency earthquake swarms, *Nature*, *446*, 305–307, doi:10.1038/nature05666.

Shelly, D. R., W. L. Ellsworth, T. Ryberg, C. Haberland, G. S. Fuis, J. Murphy, R. M. Nadeau, and R. Bürgmann (2009), Precise location of San Andreas Fault tremors near Cholame, California using seismometer clusters: Slip on the deep extension of the fault?, *Geophys. Res. Lett.*, *36*, L01303, doi:10.1029/2008GL036367.

Song, T.-R. A., D. V. Helmberger, M. R. Brudzinski, R. W. Clayton, P. Davis, X. Pérez-Campos, and S. K. Singh (2009), Subducting slab ultra-slow velocity layer coincident with silent earthquakes in southern Mexico, *Science*, *324*, 502–506, doi:10.1126/science.1167595.

Thomas, A. M., R. Bürgmann, and D. S. Dreger (2013), Incipient faulting near Lake Pillsbury, California, and the role of accessory faults in plate boundary evolution, *Geology*, *41*, 1119–1122, doi:10.1130/G34588.1.

Thurber, C. H., X. Zeng, A. M. Thomas, and P. Audet (2014), Phase-weighted stacking applied to low-frequency earthquakes, *Bull. Seismol. Soc. Am.*, *104*, 2567–2572, doi:10.1785/0120140077.

Verdonck, D., and G. Zandt (1994), Three-dimensional crustal structure of the Mendocino Triple Junction region from local earthquake travel times, *J. Geophys. Res.*, *99*, 23,843–23,858.

Waldhauser, F., and D. P. Schaff (2008), Large-scale relocation of two decades of Northern California seismicity using cross-correlation and double-difference methods, *J. Geophys. Res.*, *113*, B08311, doi:10.1029/2007JB005479.

Yamashita, T. (2013), Generation of slow slip coupled with tremor due to fluid flow along a fault, *Geophys. J. Int.*, *193*, 375–393, doi:10.1093/gji/ggs117.